Pergamon

Scripta Metallurgica et Materialia, Vol. 33, No. 1, pp. 93-99, 1995

0956-716X/95 $9.50 + .00

0956-716X(95)00100-X

EXPERIMENTAL INVESTIGATION OF THERMALLY INDUCED PLASTIC DEFORMATION IN MMCS USING BACK SCATTERED KIKUCHI METHOD

S. Mukherjee H. Garmestani N. Chandra
Department of Mechanical Engineering, FAMU/FSU College of Engineering,
Florida A&M University, Florida State University
Tallahassee, FL 32316-2175, U.S.A.

(Received December 5, 1994)
(Revised February 17, 1995)

Introduction

Electron back scattered patterns (EBSP) have been successfully used in measuring crystal orientations in polycrystalline bulk samples. Application of this technique for local strain measurements are still in developmental stages. In this work, the electron back scattered Kikuchi patterns are being used to measure residual stresses in composite specimens with very high spatial resolution. Such measurements are important in composite materials since sharp stress gradients occur in regions of the order of a few microns. Techniques such as X-ray and neutron diffraction can yield only average values of stresses over large regions as the area of interrogation in these techniques, at very best, span a few hundred microns. Back scattered Kikuchi Diffractometry (BKD), which obtains EBSPs in a scanning electron microscope, has the potential to capture large inelastic strains and hence stress gradients in a narrow region. A considerable amount of theoretical work [1–2] has shown that large stress gradients are generated near the fiber-matrix interface of metallic/intermetallic matrix composites during processing, which in turn influence their strength and stiffness properties. The results have also shown that interfacial shear properties are greatly affected by residual stresses [3]. Since all other stress measurement techniques do not have the required spatial resolution of a few microns, at present there are no direct experimental observations of the sharp stress gradient near the interface. The purpose of this investigation is to use the BKD technique to examine the presence of process induced thermal stress gradient near the fiber-matrix interface in metal matrix composites.

Tungsten fiber reinforced composite was selected with pure aluminum as the matrix material. The selection of a pure matrix material removes some of the inhomogeneity problems faced by earlier investigators, since particulate inclusions disturb the local inelastic strain pattern rendering the interpretation of the experimental results difficult. We also chose to analyze a region within the composite where the fibers are non-uniformly spaced. Since the thermal residual stress in the matrix is a function of fiber-to-fiber spacing, different radial paths between the fibers are subjected to different levels of process induced residual stresses. In this paper, we first present numerical results of processing induced residual stresses in Al-W composite using finite element method. Experimental methods of evaluation of BKD patterns are

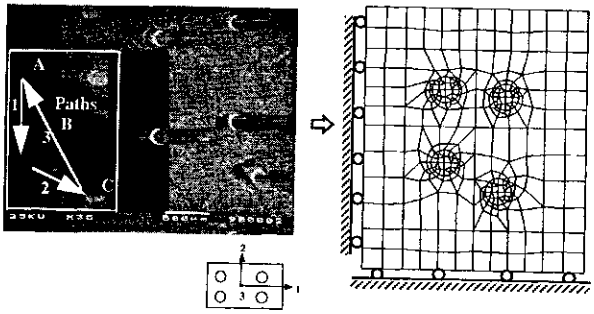

Figure 1. Photomicrograph of Al-W Composite and FEM discretization

discussed next; the details of extracting quantitative information from these patterns using image analysis are also given. Comparison between the numerical results and experimental data are made and it is clearly shown that sharp stress gradients do exist near the fiber-matrix interfaces of metal matrix composites as a result of processing.

Process Induced Residual Stresses

The composite material used in this study comprised of tungsten fibers reinforcing a pure aluminum matrix. As-processed composite material was soaked at 370°C in an argon atmosphere and then allowed to cool slowly down to room temperature. It is assumed that the composite is stress free during soaking. The region studied is shown in Figure 1, along with the finite element mesh discretization of the same region to exact scale. This region allows us to obtain a spatial distribution of stresses which are not radially symmetric. The matrix and fiber material properties are given in Figure 2. Fiber is assumed to remain elastic, whereas the matrix is assumed to be elastic-perfectly plastic with yield strength and Young's modulus changing with temperature. Three different paths 1, 2 and 3 are shown in the figure, where detailed analyses were made. It will be shown later that path 3 was used as a calibration curve for determining inelastic strain, against which paths 1 and 2 were compared.

The non-uniform region was analyzed using the finite element method to determine the distribution of process induced residual stresses. Since the region is non-uniform, a representative unit cell for the domain

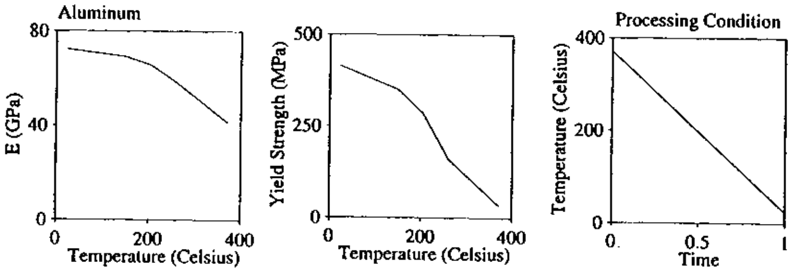

Tungsten

E (GPa)	ν	α (/ °C)
344.7	0.28	4.5E-06

Aluminum

ν	α (/ °C)
0.33	24.3E-06

Figure 2. Material properties and processing conditions

cannot be defined. For modeling purposes, the region of interest along with a buffer zone was embedded in a composite material with smeared properties computed using the method developed by Hashin [4]. The discretization of the domain and the boundary conditions are shown in the Figure 1. A finer mesh was used near the interface region to capture the stress gradients more accurately. The left edge of the domain was constrained to move only along y-axis, and the bottom edge was allowed to move only along the x-axis. The analysis was performed using finite element software ABAQUS [5]. The composite was cooled from an assumed stress-free temperature of 370°C to room temperature. An incremental elastic-plastic analysis incorporating the temperature dependent material properties reveals the presence of yielded zones near the interface. The equivalent plastic strain was determined along the three paths under investigation for the purposes of comparison with experimental data. The strain values were then normalized with respect to the peak value. Path 3 which had the highest peak value then served as a calibration curve relating the experimentally evaluated spectrum coefficients and inelastic strain.

EBSP Measurement and Analysis

Al-W composite specimens, subjected to the above heating cycle, were polished to 600 grit followed by electropolishing at room temperature to achieve relatively flat surfaces free from damage caused during the mechanical polishing. The electropolishing solution was made of a mixture of 800 ml ethanol, 140 ml distilled water and 60 ml perchloric acid. The cathode used was of stainless steel. Voltage and current used were 15V and 0.55 amperes respectively. Specimens were placed inside the SEM immediately after electropolishing to prevent surface contamination by the atmosphere.

Kikuchi patterns were imaged onto a phosphor screen and were captured using a low light CCTV camera. Three paths 1, 2 and 3 were traversed on the specimens along the same direction as the paths used in the FEM analysis. As will be shown later, image analysis forms an integral step in obtaining not only quantitative information about a specific image, but also in comparing such information against a standard. Consistent method of capturing images is very critical in order to relate the pattern to a specific inelastic strain value. The image quality is a function of dislocation density which in turn depends on the magnitude of local inelastic strain. In an earlier work, Wilkinson and Dingley[7] used patterns from Al 6061 specimens subjected to different levels of plastic strain and then later used them as basis for relating the degree of plastic strain in an Al-Silicon carbide composite material. However, he faced great difficulty in comparing two sets of images obtained under varying conditions. In the present work, we devised methods to obtain images under almost identical external conditions, thus leaving only the material state of strain to change the image quality.

Some of the problems associated with comparing two different BKD patterns are discussed below. For the purpose of consistent image acquisition, we established a background image pattern by capturing a picture of the phosphor screen at low magnification. This background was then used in a hardware subtraction to obtain the final pattern. It is difficult to use the same background for all specimens. Also factors such as filament current, and brightness and contrast settings in an image capture software can induce non-linear effects in images which cannot be nullified. If these effects are not taken into consideration inaccurate results are obtained. We attempted to eliminate some of these problems by using the same specimen for calibration and keeping brightness, contrast and background constant over a path and capturing experimental data in a single sitting.

A preliminary qualitative comparison was made on different poles and as a result it was found that the ⟨112⟩ and the ⟨011⟩ poles showed substantial changes in image quality and were chosen for further analysis. The BKD patterns corresponding to ⟨112⟩ and ⟨011⟩ poles were captured in the aluminum matrix at fairly regular intervals along each of the three paths from one fiber-matrix interface to another. Figure 5 shows a typical raw BKD picture obtained along one of the paths at near an interface, in the matrix and near the opposite end of the path in the other interface. It can be seen that the image gets sharper as one moved away from either of the interfaces and the sharpest images are always obtained at matrix locations in the middle of two fibers. It should be pointed out that a perfectly aligned crystal devoid of any dislocation produces an extremely sharp BKD pattern, and the sharpness decreases with dislocation density. Thus this sharpness decline can be related to changes in the value of equivalent plastic strain. The pictures were then analyzed with a data processing software called EXPLORER on a Silicon Graphics Indigo computer.

Image Analysis

The change in image quality (diffusivity) can be estimated using a 1-D fourier transform analysis, as suggested by Dingley [6–7]. However, such an analysis involves the selection of a specific pole, averaging the transform across the bands around the pole, and then averaging these values over several pictures. It is noticed that this process involves averaging over widely ranging values of data and thus involves a large error band. In this work, we have used a 2-D fourier transform analysis which eliminates the averaging process from the analysis. The 2-D fast fourier transform is in essence a frequency analysis of the image which can be described as a set of sine waves of varying frequency. The higher the frequency of the sine wave the finer the detail. As the pattern becomes more diffuse i.e. the contrast of the image decreases, the amplitude of the higher frequencies of the transform should decrease and, in principle the relative magnitude of the high to low frequency contributions will be a measure of the diffusiveness of the pattern [8].

The raw images were not subjected to image enhancement procedures like histogram modification or filtering as these procedures were found to alter the gray scale values in a non-linear way. Such variations may be erroneously interpreted as arising due to inelastic strain. The first step in the analysis is to mask a square region comprising of 120x120 pixels centered around a pole and extract this region from the picture. The region is then digitized in terms of gray scale values corresponding to every pixel in the region. The matrix containing the gray scale intensity information is then subjected to a 2-D fast fourier transform. Once the transform values have been determined, the spectrum which is the magnitude of the fourier transform is computed. The spectrum is plotted in the frequency domain and a surface plot is obtained. The area under the surface of the first peak along with the total area under the surface of the spectrum is then determined, as schematically shown in Figures 3 and 4. The spectrum coefficient SC, can now be defined as

$$SC = \frac{\text{Area under the first peak}}{\text{Total area under the surface of the spectrum}}$$

which gives a measure of the diffusivity of the picture. The highest value of the spectrum coefficient was found on the path 3 which is our calibration path. The peak value was used to normalize the spectrum coefficients of all the other BKD pattern data so that the values of the spectrum coefficient were in the range from 0 to 1. The distances between fibers were also normalized, and the normalized values of the spectrum coefficients were plotted against the normalized distance between fibers for the three different paths. Figure 7 shows the results from the experiments along with the computed results for the plastic strain distribution.

Results and Discussion

Figure 6 shows the computed plastic strain distribution resulting from process induced residual stresses, from a stress free temperature of 370°C. Using the procedure outlined earlier, the spectrum coefficients

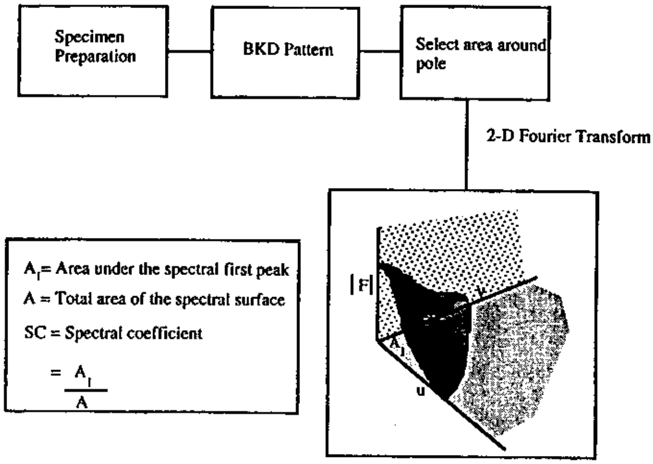

Figure 3. Image analysis procedure

were evaluated at each of the material points, after subjecting the pattern to identical image analysis procedures. We believe that the spectrum coefficients in the constrained matrix material (in the composite) will be different from that of a homogeneous state obtained in a uniaxial tensile test. A normalization curve was established between the computed maximum and minimum plastic strain and the maximum and minimum normalized spectrum coefficients obtained using BKD data in path 3. This normalization enables us to correlate the computed interfacial plastic strain qualitatively to the measured BKD data near the same material point. It can be seen that the gradients of plastic strain are clearly very steep as shown in experimental measurements. Thus it verifies the existence of very sharp gradients of strain (and hence stress) as predicted by numerical and analytical models. Near the interfaces of both fibers in a path, the BKD data show a high value of plastic strain and as we move into the matrix away from the interface, there is a steep reduction in the strain and the curves flatten out.

The normalization obtained in path 3 was applied to path 1 and 2. We should note that the plastic strain variation is not the same as the fiber spacing is non-uniform and the radial path lengths are different. The comparisons between FEM and BKD are shown in Figures. 7(a), 7(b) and 7(c). Reasonably good agreement is seen. Once again the sharp gradients of strain (and hence stress) are clearly seen in the two cases.

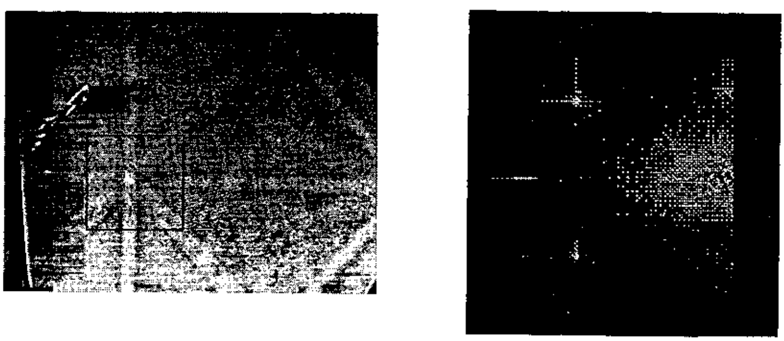

BKD pattern 2-D Fourier spectrum

Figure 4. Spectrum analysis of a BKD pattern

Near interface of first fiber (A of fig. 1) | Near center (B of fig. 1) | Near interface of second fiber (C of fig. 1)

Figure 5. Typical variations in BKD sharpness with radial distance between fibers

Summary

We have used the BKD method to investigate the predicted stress gradients, induced near the fiber-matri interfaces during the processing of metal matrix composites. The BKD patterns in a composite specime have to be acquired with great consistency before the images can be analyzed for quantitative informatio on dislocation densities and hence plastic strain. We have developed a suitable image acquisition an analysis procedure for this purpose. The developed methodology has been applied to evaluate the plasti strain gradients in an Al-W composite subjected to a cooling cycle. We have compared the BKD results t FEM analysis which takes into account the temperature dependent material properties and actual spatia distribution of fibers. The results reveal the presence of sharp gradients of plastic strain near the interface:

Acknowledgments

The authors wish to acknowledge NASA for partially funding the research effort. Also they wish to than professors B. L. Adams and D. J. Dingley for some useful discussions on the experimental techniques.

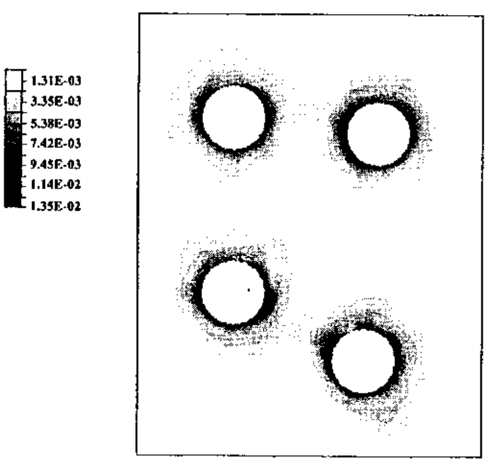

Figure 6. Equivalent plastic strain in the matrix

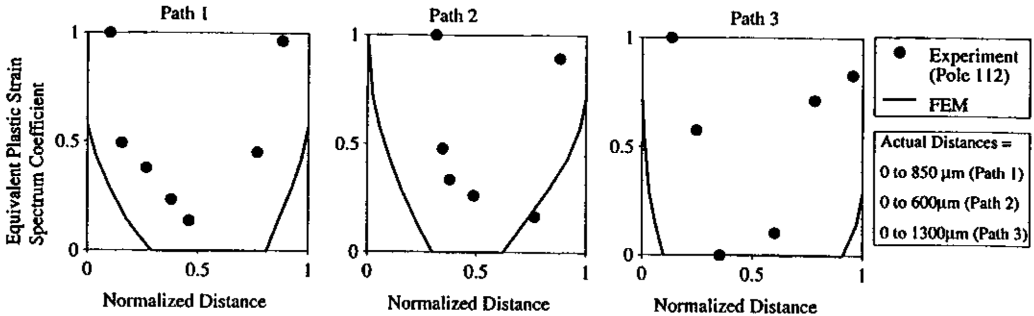

Figure 7. Variation of plastic strain along the different paths

References

1. N. Chandra, C. R. Ananth and H. Garmestani, *Journal of Composites Technology and Research*, **16**, 1, 37 (1994).
2. N. Chandra and Z. Xie, *Journal of Applied Mechanics*, (in print), (1994).
3. C. R. Ananth and N. Chandra, *Journal of Composite Materials*, (in print), (1994).
4. Z. Hashin, *Journal of Applied Mechanics*, **46**, 543 (1979).
5. ABAQUS, User Manual, (1994).
6. A. J. Wilkinson and D. J. Dingley, *Acta Metallurgica et Materiala*, **40**, 12,3357, (1992).
7. A. J. Wilkinson and D. J. Dingley, *Acta Metallurgica et Materiala*, **39**, 12,3047, (1991).
8. S. I.Wright, B.L. Adams, K. Kunze, *Material Science and Engineering*, **A160**, 2299, (1993).